Intraspecies Regulation of Ribonucleolytic Activity†

R. Jeremy Johnson,‡ Luke D. Lavis,§ and Ronald T. Raines*,‡,§

Departments of Biochemistry and Chemistry, University of Wisconsin−Madison, Madison, Wisconsin 53706

Received July 30, 2007; Revised Manuscript Received September 3, 2007

ABSTRACT: The evolutionary rate of proteins involved in obligate protein−protein interactions is slower and the degree of coevolution higher than that for nonobligate protein−protein interactions. The coevolution of the proteins involved in certain nonobligate interactions is, however, essential to cell survival. To gain insight into the coevolution of one such nonobligate protein pair, the cytosolic ribonuclease inhibitor (RI) proteins and secretory pancreatic-type ribonucleases from cow (*Bos taurus*) and human (*Homo sapiens*) were produced in *Escherichia coli* and purified, and their physicochemical properties were analyzed. The two intraspecies complexes were found to be extremely tight (bovine $K_d = 0.69$ fM; human $K_d = 0.34$ fM). Human RI binds to its cognate ribonuclease (RNase 1) with 100-fold greater affinity than to the bovine homologue (RNase A). In contrast, bovine RI binds to RNase 1 and RNase A with nearly equal affinity. This broader specificity is consistent with there being more pancreatic-type ribonucleases in cows (20) than humans (13). Human RI (32 cysteine residues) also has 4-fold less resistance to oxidation by hydrogen peroxide than does bovine RI (29 cysteine residues). This decreased oxidative stability of human RI, which is caused largely by Cys74, implies a larger role for human RI as an antioxidant. The conformational and oxidative stabilities of both RIs increase upon complex formation with ribonucleases. Thus, RI has evolved to maintain its inhibition of invading ribonucleases, even when confronted with extreme environmental stress. That role appears to take precedence over its role in mediating oxidative damage.

The discovery of extensive protein−protein interaction networks has informed investigations of protein evolution (*1*−*3*). For example, the rate of evolution within a protein−protein interaction network has been found to depend on the number of binding partners, the concentration of each protein, and the evolutionary age of the proteins (*4*−*10*). These relationships extend to subclasses of interactions, as obligate protein−protein interactions, which are defined as interactions necessary for the stability of an individual protein (*11*), evolve at a slower rate, and show a greater degree of coevolution than do nonobligate interactions, which are interactions between proteins that can remain stable independently (*7*). Nonetheless, the coevolution of certain nonobligate protein−protein interactions, such as particular receptor−ligand and enzyme−inhibitor interactions, can be essential for cell survival (*11*). To understand the coevolution of such a nonobligate pair, we have investigated the complex formed between the cytosolic ribonuclease inhibitor protein (RI[1]) and secretory pancreatic-type ribonucleases, as failure to inhibit the enzymatic activity of an invading ribonuclease can lead to cell death (*12*−*15*).

The ribonuclease A superfamily is composed of homologues of bovine pancreatic ribonuclease (RNase A (*12*); 124 residues; EC 3.1.27.5), which are found only in vertebrates (*16*−*20*). The superfamily has expanded rapidly (*21*, *22*), with only three members in fish (*Danio rerio*) (*23*) and chicken (*Gallus gallus*) (*21*, *24*) but 20 and 13 members in cow (*Bos taurus*) (*22*) and human (*Homo sapiens*) (*21*), respectively. The lethal enzymatic activity of ribonucleases is modulated by RIs (*25*, *26*), which binds to some members of the ribonuclease A superfamily with affinities in the femtomolar range (*27*, *28*). RI is able to exert this affinity using its large concave surface area (*28*−*30*), even though the sequence identity among superfamily members is <30% (*26*, *28*). RI evolved rapidly by exon duplication around the time of ribonuclease expansion (*31*), suggesting coevolution of the protein families, but this direct relationship has not been demonstrated conclusively (*26*).

Although RNase A is perhaps the most studied of all enzymes (*12*), little is known about its cognate inhibitor,

† This work was supported by Grant CA73808 (NIH). R.J.J. and L.D.L. were supported by Biotechnology Training grant 08349 (NIH). L.D.L. was also supported by an ACS Division of Organic Chemistry Fellowship, sponsored by the Genentech Foundation. The Biophysics Instrumentation Facility was established with grants BIR-9512577 (NSF) and RR13790 (NIH). The W.M. Keck Center for Chemical Genomics was established by a grant from the W.M. Keck Foundation.

* To whom correspondence should be addressed: Department of Biochemistry, University of Wisconsin−Madison, 433 Babcock Dr., Madison, WI 53706-1544. Tel: 608-262-8588. Fax: 608-262-3453. E-mail: raines@biochem.wisc.edu.

‡ Department of Biochemistry.

§ Department of Chemistry.

[1] Abbreviations: BSA, bovine serum albumin; bRI, bovine ribonuclease inhibitor; CD, circular dichroism; cDNA, complementary DNA; DTT, dithiothreitol; HEPES, *N*-cyclohexyl-2-aminoethanesulfonic acid; hRI, human ribonuclease inhibitor; LRR, leucine-rich repeats; MALDI−TOF, matrix-assisted laser desorption/ionization−time-of-flight; MES, 2-(*N*-morpholino)ethanesulfonic acid; PBS, phosphate-buffered saline; PCR, polymerase chain reaction; PDB, Protein Data Bank; RI, ribonuclease inhibitor; RNase A, bovine pancreatic ribonuclease; RNase 1, human pancreatic ribonuclease.

10.1021/bi701521q CCC: $37.00
Published on Web 10/23/2007

bovine RI (bRI; 456 residues). In contrast, human RI (hRI; 460 residues) is known to bind to ribonucleases from such evolutionary distant organisms as fish, chickens, and cows (*23*, *24*, *29*, *30*). Yet, we demonstrated recently that the affinity of hRI for RNase A is significantly lower than that for human pancreatic ribonuclease (RNase 1; 128 residues), suggesting a coevolution of affinity between RI and its species-specific ribonucleases (*28*).

Here, we report on the heterologous production, purification, and characterization of bRI. We find that bRI forms a highly stable complex with both RNase A and RNase 1. We also find that bRI is stabilized to both thermal and oxidative stress upon ribonuclease binding. These and other observations provide insight into the molecular evolution and biological imperatives of an extraordinary nonobligate protein−protein interaction.

EXPERIMENTAL PROCEDURES

General. Escherichia coli BL21(DE3) cells and the plasmid pET22b(+) were from Novagen (Madison, WI). DNA oligonucleotides for PCR, sequencing, and mutagenesis were from Integrated DNA Technologies (Coralville, IA). Protein purification columns were from GE Healthcare (Piscataway, NJ). MES buffer (Sigma Chemical, St. Louis, MO) was purified by anion−exchange chromatography to remove trace amounts of oligomeric vinylsulfonic acid (*32*). Restriction and PCR enzymes were from Promega (Madison, WI). All other chemicals were of commercial grade or better and were used without further purification.

Terrific broth (TB) contained (in 1.00 L) tryptone (12 g), yeast extract (24 g), glycerol (4 mL), KH_2PO_4 (2.31 g), and K_2HPO_4 (12.54 g). Phosphate-buffered saline (PBS), pH 7.4, contained (in 1.00 L) NaCl (8.0 g), KCl (2.0 g), $Na_2HPO_4 \cdot 7H_2O$ (1.15 g), KH_2PO_4 (2.0 g), and NaN_3 (0.10 g).

Circular dichroism (CD) data were collected with a model 62A DS CD spectrometer (Aviv, Lakewood, NJ) equipped with a temperature controller. The molecular mass of each RI and ribonuclease was determined by matrix-assisted laser desorption/ionization−time-of-flight (MALDI−TOF) mass spectrometry using a Voyager-DE-PRO Biospectrometry Workstation (Applied Biosystems, Foster City, CA). CD and MALDI−TOF mass spectrometry experiments were performed at the campus Biophysics Instrumentation Facility. The fluorescence intensity in microtiter plates was recorded in a Perkin−Elmer EnVision 2100 plate reader equipped with an FITC filter set (excitation: 485 nm with a 14-nm bandwidth; emission: 535 nm with a 25-nm bandwidth; dichroic mirror cutoff: 505 nm) in the campus W. M. Keck Center for Chemical Genomics.

RI cDNA Cloning and Protein Preparation. The sequence of bRI was identified by its hypothetical annotation in the GenBank database (http://www.ncbi.nlm.nih.gov/Genbank/index.html). bRI (gi:78369509) was labeled as "*Bos taurus* similar to ribonuclease inhibitor". Its amino acid sequence had 74% identity to that of hRI (Figure S-1) (*28*). DNA primers 5′-CTTTTCATATGAAGCTGGACATCCAGTGTGAGCAGCTCAGCG-3′ and 5′-CTTTTTAAGCTTTCAGGAGATGATCCGCAGGCCAGGCTTGCTCTC-3′ were designed to amplify the cDNA encoding bRI and to incorporate *Nde*I and *Hind*III restriction sites at the 5′ and 3′ ends, respectively. cDNA encoding bRI was amplified by PCR from a bovine brain cDNA library (BioChain Institute, Hayward, CA). The PCR product was inserted into plasmid pCR4-TOPO (Invitrogen, Carlsbad, CA), and sequence analysis was performed to ensure proper amplification.

RI Production and Purification. The cDNA encoding bRI was inserted into plasmid pET22b(+) for protein production. A plasmid that encodes hRI (*28*, *33*) was used to create cysteine-residue variants of hRI using the Quikchange site-directed mutagenesis kit (Stratagene, La Jolla, CA). Both wild-type RI proteins and variants of hRI were produced and purified by using the procedure described previously (*28*, *34*).

Ribonuclease Production, Purification, and Labeling. RNase 1, RNase A, and their free cysteine residue variants were purified from inclusion bodies using the oxidative folding procedure described previously (*28*, *33*). Plasmids containing DNA encoding wild-type RNase 1 and RNase A were used to create variants with a free cysteine residue at position 19 (*28*, *35*) using the Quikchange site-directed mutagenesis kit (Stratagene, La Jolla, CA). Position 19 was chosen as the attachment site, because attachment of fluorescent groups at this position does not have a detectable effect on the ribonucleolytic activity or RI-affinity of the resulting variants (*25*, *36*). Variants of RNase 1 and RNase A with a free cysteine were initially protected by reaction with 5,5′-dithio-bis(2-nitrobenzoic acid) (*28*, *35*, *37*). Immediately before fluorophore attachment, protected variants were deprotected by using a 3-fold molar excess of dithiothreitol (DTT) and desalted by chromatography using a PD-10 desalting column (Amersham Biosciences, Piscataway, NJ). Deprotected ribonuclease variants were reacted for 4−6 h at 25 °C with a 10-fold molar excess of 2′,7′-diethylfluorescein-5-iodoacetamide, which was synthesized as described previously (*38*). Diethylfluorescein-labeled ribonucleases were purified by chromatography using a HiTrap SP FF column.

Dissociation Rate. The dissociation rates of the RI·ribonuclease complexes were determined by using a procedure described previously (*28*). Briefly, diethylfluorescein-labeled ribonuclease (100 nM) in PBS containing tris(2-carboxyethyl)phosphine (0.10 mM) and bovine serum albumin (BSA, 0.10 mg/mL; Sigma Chemical) was added to a 96-well microtiter plate, and the initial fluorescence was measured. RI was then added at equimolar concentrations (100 nM) and incubated with a labeled ribonuclease at 25 °C for 5 min. A 50-fold molar excess of human angiogenin (5 μM) (purified as described previously (*39*)) was added to scavenge dissociated RI, and the change in fluorescence was measured at various time points. To ensure that the stability of the proteins was maintained over the extended duration of the experiment, additional data points were monitored under the same conditions, only without the addition of angiogenin. Data are the mean (±SE) of six replicates standardized for the mean fluorescence of six replicates of a rhodamine 110 standard (10 nM) and normalized for the fluorescence before RI addition (F_∞) and for the maximum fluorescence change of the fully dissociated hRI·RNase A complex. Fluorescence data were fitted to eq 1 with the program GraphPad Prism 4.02 (GraphPad Software, San Diego, CA) to determine the dissociation rate (k_d), wherein F_0 is the fluorescence before the addition of angiogenin, and F_∞ is the fluorescence before RI addition.

Initial fluorescence data (<4 h) were not included in the analysis of RI·RNase 1 complexes, as they showed a rapid burst in fluorescence similar to that observed in previous dissociation rate determinations (*27*, *28*). Initial fluorescence data were, however, included in the analysis of the RI·RNase A complexes, as the fluorescence change for their dissociation was greater than the initial burst.

$$F = F_0 + (F_\infty - F_0)(1 - e^{k_d t}) \quad (1)$$

Conformation and Conformational Stability. CD spectroscopy was used to assess the secondary structural conformation of RI·ribonuclease complexes (*40*). Complexes between RI (25 μM) and ribonuclease (28 μM) were formed by incubation in PBS containing DTT (2 mM) at 25 °C for 30 min. A slight molar excess of ribonuclease was added to ensure that all RI molecules were complexed with ribonuclease. The CD signal contributed by the excess ribonuclease was then masked by the higher CD signal from RI. Additionally, free ribonuclease (28 μM) and free RI (25 μM) were prepared for CD measurement using conditions identical to those used to prepare RI·ribonuclease complexes. CD spectra were acquired from 260 to 205 nm in 1-nm increments at 25 °C, and the background CD spectrum of PBS containing DTT (2 mM) was subtracted from each spectrum. CD spectra are shown as the mean residue-weight ellipticity at each wavelength (*41*).

CD spectroscopy was also used to evaluate the conformational stability of the RI·ribonuclease complexes (*40*). The preparation of free RI, free ribonuclease, and RI·ribonuclease complexes was the same as for CD spectra determination. Protein solutions were heated from 25 to 75 °C in 2-°C increments. The change in molar ellipticity at 222 nm was measured after a 2-min equilibration at each temperature. CD data at 222 nm were fitted to a two-state model with the program GraphPad Prism 4.02 to determine the values of T_m (*42*, *43*).

Oxidative Stability. The stability of RI and RI·ribonuclease complexes to oxidation by hydrogen peroxide (H_2O_2) was assessed by using a method similar to that described previously (*44*), except that the decrease in the fluorescence of diethylfluorescein-labeled ribonuclease upon RI-binding was used to quantitate binding instead of indirectly following RI-binding through measurement of ribonucleolytic activity (*36*, *38*). Immediately prior to assaying oxidative stability, purified RI was dialyzed for 16 h at 4 °C against 20 mM HEPES−HCl buffer, pH 7.6, containing KCl (50 mM) and DTT (200 μM), such that the final concentration of DTT in the H_2O_2 reactions was ≤50 μM. Fresh H_2O_2 (30% v/v, Fisher Scientific, Fair Lawn, NJ, or Sigma Chemical) was diluted to 2% v/v in 20 mM HEPES−HCl buffer, pH 7.6, containing KCl (50 mM) (Buffer A). The H_2O_2 solution (2% v/v) was then serially diluted (10 solutions of 56:100) with Buffer A (final range = 1−0.003% v/v H_2O_2). Complexes were formed between RI (10 μM) and ribonuclease (10 μM) in Buffer A and incubated for 15 min at 23 °C prior to H_2O_2 treatment. Free RI and ribonuclease were treated identically with the same volume of Buffer A. H_2O_2 dilutions (5 μL) and RI, ribonuclease, or RI·ribonuclease complex (5 μL of a 10 μM solution) were added jointly to a 96-well PCR plate (Bio-Rad Laboratories, Hercules, CA). Plates were heated at 37 °C for 30 min in a PTC-100 thermal cycler equipped with a heated lid (Bio-Rad Laboratories). After 30 min, Buffer A (10 μL) was added to RI·ribonuclease complex and ribonuclease wells, RNase 1 (10 μL of a 5 μM solution) was added to hRI wells, and RNase A (10 μL of a 5 μM solution) was added to bRI wells. Plates were incubated for an additional 5 min in the thermocycler at 37 °C, and an aliquot (8 μL) from each well was then added to PBS (392 μL, Invitrogen, Grand Island, NY) containing BSA (0.10 mg/mL) and DTT (5 mM). To quantitate the fluorescence change upon RI-binding, an aliquot (100 μL) from the PBS dilution was transferred to a 96-well black nonbinding surface polystyrene plate (Corning, Corning, NY). Data were converted to the fraction of RI oxidized by normalizing for the fluorescence of the unbound complex and were fitted to eq 2 to determine IC_{50} values. The fluorescence intensity of diethylfluorescein-labeled ribonucleases remained constant over the range of H_2O_2 concentrations used in the assay, indicating that any change observed was not due to an effect of H_2O_2 on the fluorophore or free ribonuclease.

$$y = \frac{100\%}{1 + 10^{(\log(IC_{50}/[H_2O_2]))^h}} \quad (2)$$

Sequence and Phylogenetic Analysis. Sequence alignments of RI and ribonuclease (Figure 1 and Figures S-1−S-3) were performed with the program Clustal W (*45*). Cladograms of RI and ribonuclease were made with the program MegAlign in the Lasergene software package (DNASTAR, Madison, WI). Bootstrap values were calculated by using 2000 replicates and values >40 are reported. Accession codes for RI sequences used for alignment are *Bos taurus* (gi: 78369509), *Rattus norvegicus* (gi: 77416905), *Mus musculus* (gi: 78099143), *Gallus gallus* (gi: 57529989), *Sus scrofa* (gi: 1942101), *Pan troglodytes* (gi: 38503347), and *Homo sapiens* (gi: 71042211). Accession codes for ribonuclease sequences used for alignment are *Bos taurus* brain (gi: 27806923), *Bos taurus* seminal (gi: 32441267), *Bos taurus* pancreatic (gi: 48429071), *Rattus norvegicus* (gi: 71361661), *Mus musculus* (gi: 133221), *Gallus gallus* (gi: 45383972), *Sus scrofa* (gi: 133225), *Pan troglodytes* (gi: 38503271), *Homo sapiens* (gi: 71042210).

RESULTS

With their large concave surface areas, the structural family of leucine-rich repeats (LRRs), for which RI is the prototype, is well-suited to recognize diverse ligands (Figure 1A) (*46*). Accordingly, RI has served as a structural model for protein−protein recognition (*26*). Multiple biological roles have been assigned to RI, including protecting cells from rogue ribonucleases and scavenging free radicals (*25*, *26*, *47*, *48*). The latter activity is attributed to the 29−32 free cysteine residues found in RI, whose oxidation leads to irreversible inactivation of the protein (*44*, *49*).

The amino acid sequences of RIs from multiple organisms (Figure S-2) have been reported, and some of these proteins have been characterized (*50*−*54*). In 1980, bRI was isolated and found to inhibit ribonucleolytic activity (*50*). Its amino acid sequence and biochemical characteristics were, however, not reported (*47*, *50*). The amino acid sequence of bRI (Figure 1B) was annotated in the GenBank registry as "*Bos taurus* similar to ribonuclease inhibitor" (gi:78369509). The sequence of bRI was 74% identical to hRI (Figure S-1) and

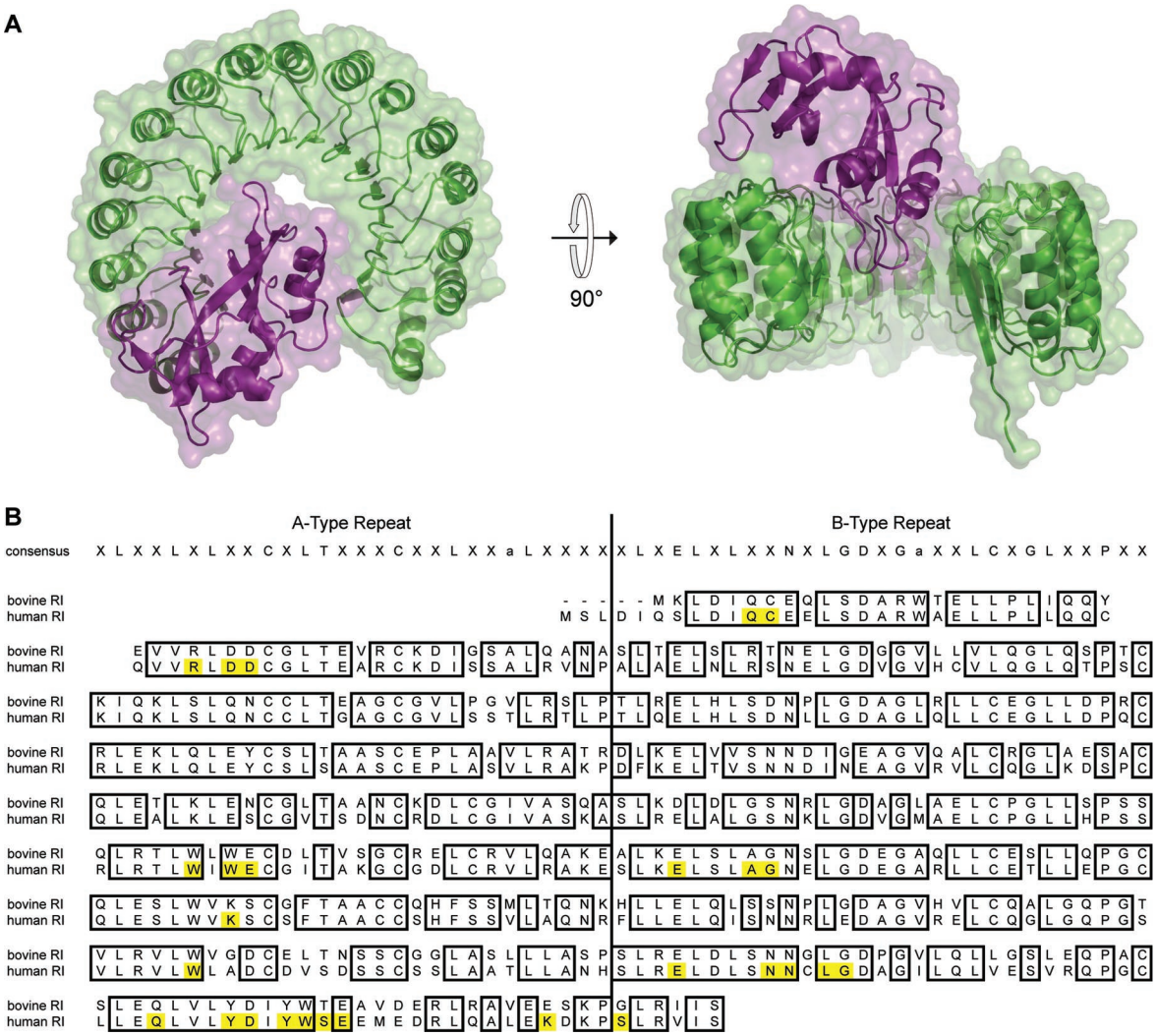

FIGURE 1: Structure and sequence of RI. (A) Ribbon diagram of the hRI (green)·RNase 1 (purple) complex (chains Y and Z from PDB accession code 1Z7X) (*28*). Images were made with the program PyMOL (DeLano Scientific, South San Francisco, CA). (B) Sequence alignment of the protein sequences of bRI and hRI. Conserved amino acids are shown with black boxes and contact residues (<3.9 Å) within the hRI·RNase 1 complex are shaded yellow (chains Y and Z from PDB accession code 1Z7X) (*28*). Alignments were performed with the program Clustal W (*45*). Consensus sequences for A-Type and B-Type repeats of RI-like LRRs were adapted from ref *26*.

had the consensus A-Type and B-Type repeating architecture of RIs (Figure 1B) (*26*). bRI contains 29 of the 32 cysteine residues in hRI and was able to be produced and purified by a procedure identical to that used for hRI (*28*, *34*), yielding 5 mg of bRI per liter of *E. coli* culture. bRI, hRI, and their complexes with RNase A and RNase 1 were then analyzed to reveal environmental factors that influence complex-stability and thereby modulate the regulation of ribonucleolytic activity.

Dissociation Rate for RI·Ribonuclease Complexes. The RI·ribonuclease complex is one of the tightest known biological interactions (*27*, *28*, *55*). The association rate constant for complex formation between RI and ribonucleases is close to the diffusion limit (10^9 M^{-1} s^{-1}) (*27*, *28*, *56*), due to the strong electrostatic nature of the interaction (*28*, *57*). Yet, the dissociation rate constants of the hRI·RNase 1 and hRI·RNase A complexes differ significantly, owing to differences in the hydrogen bonds and van der Waals contacts made between hRI and the two ribonucleases (*28*).

The dissociation rate constants for the complexes of bRI and hRI with RNase A and RNase 1 were determined by using a competition assay described previously (*27*, *28*). The observed increase in fluorescence as the RI·ribonuclease complex dissociates is shown in Figure 2, and the k_d values determined by fitting the resulting data to eq 1 are listed in Table 1. Only the hRI·RNase A complex dissociated completely over the length of the experiment (Figure 2A) with a $t_{1/2}$ (= ln $2/k_d$) of 14 h, which is nearly identical to the value determined previously (13 h) (*27*). All of the other RI·ribonuclease complexes were <50% dissociated after 15 days (Figure 2). Their k_d values were within 2-fold of each other (Table 1), and their $t_{1/2}$ values (34 days for bRI·RNase A, 78 days for bRI·RNase 1, and 68 days for hRI·RNase 1) were within 2-fold of that for the hRI·angiogenin complex ($t_{1/2}$ = 60 days) (*27*). The clustering of the k_d values of the most stable RI·ribonuclease complexes suggests that an upper limit for the half-lives of the dissociation rate of an RI·ribonuclease complex has been reached at approximately 3 months (Table 1) (*27*).

By assuming that all of the complexes have association rate constants close to the diffusion limit (*28*), the equilibrium dissociation constants (K_d) of the complexes can be estimated. The K_d values for the bRI·RNase A, bRI·RNase 1, and hRI·RNase 1 complexes are all in the range of 0.30−

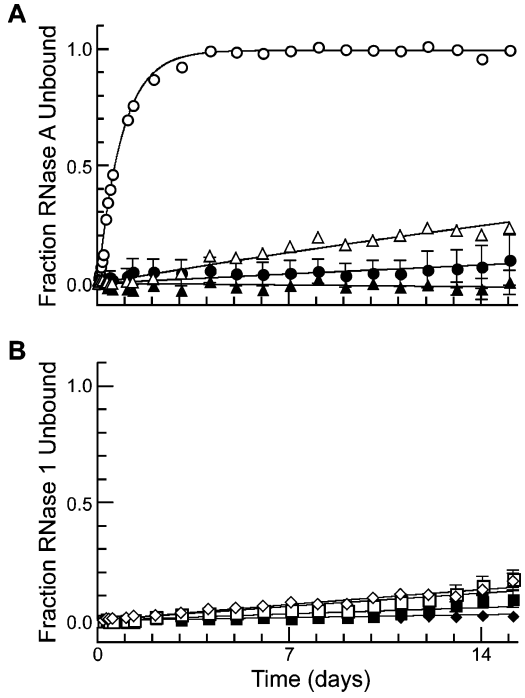

FIGURE 2: Dissociation of RI·ribonuclease complexes. The release of diethylfluorescein-labeled ribonuclease (100 nM) from RI (100 nM) was followed over time after the addition of a 50-fold molar excess of angiogenin (5 μM) (open symbols) or after the addition of PBS (closed symbols). Data points are the mean (±SE) of six separate measurements and are normalized for both the average fluorescence of rhodamine 110 (10 nM) and the fluorescence of unbound RNase A from hRI·RNase A. The initial fluorescence of unbound ribonuclease was used as the end-point for complete ribonuclease release (*28*). (A) Dissociation of bRI·RNase A (△) and hRI·RNase A (○). (B) Dissociation of bRI·RNase 1 (□) and hRI·RNase 1 (◇).

0.69 fM, whereas the hRI·RNase A complex has at least 50-fold lower stability (35 fM) (Table 1). Overall, both bRI and hRI are tight inhibitors of ribonucleases, but bRI binds more tightly to both human and bovine ribonucleases.

Conformation and Conformational Stability. Proteins are stabilized upon binding to small-molecule ligands (*58*−*61*) or with other proteins (*62*, *63*). The magnitude of the stabilization is often related directly to the affinity of the protein for the ligand (*59*, *61*, *64*). To determine whether the conformational stability of bRI and hRI increases upon complex formation and whether this increase correlates with complex-stability, the conformational stability of each RI·ribonuclease complex was determined by CD spectroscopy (Figure 3) (*40*, *61*, *65*).

The far-UV CD spectra of free RI, free ribonuclease, and RI·ribonuclease complexes are depicted in Figures 3A and 3C. bRI and hRI have similar CD spectra, with minima at 222 nm being indicative of similar secondary structure and three-dimensional architecture (*65*). When complexed with a ribonuclease, the maxima of the CD spectra for hRI and bRI shift to 225 nm. Complexes between RI and ribonuclease were formed with a slight molar excess of ribonuclease (28 μM) to RI (25 μM) to ensure complete complex formation by RI and to allow accurate determination of the conformational stability of RI. The ellipticity of RI, which has a repeating α-helix, β-strand architecture (Figure 1A), overwhelms the ellipticity of the ribonucleases (e.g., bRI: $[\theta]_{222\ nm} = -14\,000$ deg·cm^2·dmol^{-1}; RNase A: $[\theta]_{222\ nm} = -7600$ deg·cm^2·dmol^{-1}; Figures 3A and 3C). Hence, changes in ellipticity report largely on changes to the conformation of RI.

The stability of the RI·ribonuclease complexes as a function of temperature is shown in Figures 3B and 3D. The midpoints of each transition curve (T_m) were obtained by fitting the data to a two-state model and are listed in Table 1. Unbound hRI (T_m = 54 °C) is slightly more stable than is unbound bRI (T_m = 51 °C), but bRI gains more stability upon forming a complex with either ribonuclease. The T_m values of both RIs increase by >10 °C upon complex formation with ribonuclease. The hRI·RNase A complex was the least stable of the four complexes, in accord with it having the largest dissociation rate constant (Figure 2).

Oxidative Stability. With its 29−32 free cysteine residues and abundance in the cytosol, RI serves to mediate oxidative damage (*48*). RI scavenges reactive oxygen species such as superoxide anion, hydroxyl radical, and singlet oxygen with IC_{50} values below 10 μg/mL, making it a powerful antioxidant (*47*). To investigate the oxidative stability of bRI and hRI and to determine how complex formation affects their oxidative stability, the vulnerability of both RIs to oxidation by H_2O_2 was tested (*38*, *44*).

The binding curves obtained after incubating bRI, hRI, or RI·ribonuclease complexes with H_2O_2 are shown in Figure 4, and the IC_{50} values are listed in Table 1. The oxidative stability of hRI (IC_{50} = 0.017% v/v H_2O_2) was close to that measured previously by evaluating the inhibition of ribonucleolytic activity by hRI (0.007% v/v H_2O_2 (*44*)). The oxidative stability of bRI (29 cysteine residues; Figure 1B) was, however, 4-fold higher than that of hRI (32 cysteine residues). bRI has both of the adjacent cysteine pairs that were shown to be important to the oxidative resistance of hRI (*44*). Yet, native bRI has oxidative stability similar to that of previously characterized oxidation-resistant variants of hRI (Table 2) (*44*).

The decreased oxidative stability of hRI compared to bRI could be due to the replacement of three residues in bRI with cysteine in hRI (Figure 1). Two of these cysteine residues, Cys74 and Cys408 (hRI numbering), were especially attractive candidates for decreasing the oxidative stability. The sulfur atoms of Cys74 and Cys29 are within 6 Å and could form a destabilizing disulfide bond upon oxidation, as seen for adjacent free cysteine residues in hRI (*44*); Cys408 has the highest solvent-accessible surface area of any cysteine residue in hRI, as calculated for chain Y from PDB accession code 1Z7X with the program POPS (*66*). Both Cys74 and Cys408 in hRI were replaced with the corresponding residues in bRI, C74L, and C408G, and the oxidative stabilities of the resulting variants are shown in Figure 4C. C408G hRI appears to be more sensitive to oxidation, as its stability curve shows a steeper transition to the oxidized form. In the three-dimensional structure of the hRI·RNase 1 complex (*28*), Cys408 forms molecular contacts with Asn67 of RNase 1. As oxidative stability is measured in relation to RI-binding, substitution of Cys408 with a glycine residue could weaken the affinity for RNase 1, making hRI more susceptible to rapid oxidation. Yet, C408G hRI (IC_{50} = (0.023 ± 0.002)% v/v H_2O_2) still has near identical oxidative stability to wild-type hRI, whereas C74L hRI (IC_{50} = (0.043 ± 0.005)% v/v H_2O_2) has 2.5-fold higher oxidative stability than wild-type hRI, putting its stability

Table 1: Biochemical Parameters for bRI, hRI, and RI·Ribonuclease Complexes

	k_d (10^{-7} s^{-1})[a]	K_d (fM)[b]	T_m (°C)[c]	IC_{50} (% v/v H_2O_2)[d]
bRI	–	–	51.3 ± 0.1	0.071 ± 0.010
bRI·RNase A	2.36 ± 0.05	0.69	68.6 ± 0.3	0.30 ± 0.004
bRI·RNase 1	1.03 ± 0.07	0.30	68.0 ± 0.2	0.029 ± 0.008
hRI	–	–	54.1 ± 0.1	0.017 ± 0.004
hRI·RNase A	119 ± 2	35	64.2 ± 0.1	0.042 ± 0.016
hRI·RNase 1	1.17 ± 0.05	0.34	66.6 ± 0.2	0.028 ± 0.004

[a] Values of k_d (±SE) were determined by following the release of diethylfluorescein-labeled ribonuclease from the RI·ribonuclease complex over time and fitting the resulting data to eq 1. [b] Values of K_d (±SE) were calculated using the relationship $K_d = k_d/k_a$ and the k_a value for hRI + RNase A (*27*). [c] Values of T_m (±SE) were determined by CD spectroscopy in PBS containing DTT (2 mM). [d] Values of IC_{50} (±SE) are for the oxidative stability to H_2O_2 and were calculated with eq 2.

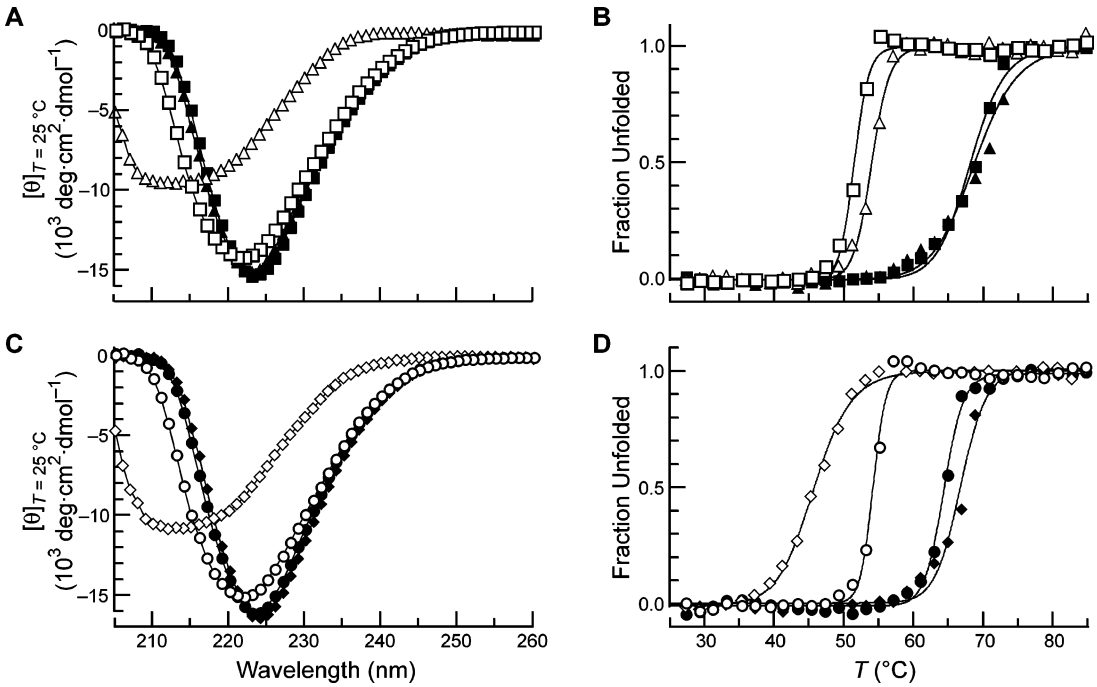

FIGURE 3: Conformation and conformational stability of RI·ribonuclease complexes. (A and C) Far-UV CD spectra of RI, ribonuclease, and RI·ribonuclease complexes (25 μM RI and 28 μM ribonuclease in PBS containing DTT (2 mM)). (B and D) Thermal denaturation of RI, ribonuclease, and RI·ribonuclease complexes (25 μM RI and 28 μM ribonuclease in PBS containing DTT (2 mM)). Molar ellipticity at 222 nm was monitored after a 2-min equilibration at each temperature. Data were fitted to a two-state model to determine values for T_m (Table 1) (*42*, *43*). Panels A and B depict data for RNase A (△), bRI (□), bRI·RNase A (▲), and bRI·RNase 1 (■); panels C and D depict data for RNase 1 (◇), hRI (○), hRI·RNase 1 (◆), and hRI·RNase A (●).

within 2-fold of that of bRI (Table 1). Thus, the existence of a cysteine residue at position 74 in hRI is responsible for the additional sensitivity of hRI to oxidation and could represent an adaptive substitution that diminishes RI concentration at a lower cytosolic reduction potential.

Upon complex formation with RNase A, bRI gains an additional 4-fold in oxidative stability and remains stably bound to RNase A at up to 0.30% v/v H_2O_2 (0.13 M H_2O_2), again underscoring the extraordinary stability of the RI·ribonuclease complex. Surprisingly, complex formation with RNase 1 elicits a 2-fold decrease in the oxidative stability of bRI. This decrease could be due to changes in the bRI structure upon RNase 1 binding, as seen upon RNase A binding to porcine RI (*29*), allowing better access to reactive sulfhydryl groups. Additionally, RNase 1, being more cationic than RNase A (*67*), could preferentially shift the pK_a of nearby cysteine residues (*38*), thereby favoring the transition from the thiol (RSH) to the more reactive thiolate (RS^-) form (*68*, *69*) and facilitating disulfide bond formation (*44*). hRI, in contrast, has slightly increased oxidative stability upon complex formation with either RNase A or RNase 1 (Table 1). Overall, the oxidative stability of RI·ribonuclease complexes seem to mirror their conformational stability.

DISCUSSION

Unregulated ribonucleolytic activity is potentially damaging to essential cellular processes (*12*, *13*, *15*, *70*). To protect themselves, cells have evolved RI (*25*, *26*, *31*). RI might have coevolved with its ribonuclease ligands (*26*, *31*), as mammalian RIs do not bind to ribonuclease homologues from frogs (*71*, *72*) and hRI has 100-fold higher affinity for human RNase 1 than for bovine RNase A (*28*). This relationship is not definitive, however, as two of three new ribonucleases identified from fish (*Danio rerio*) are bound by hRI (*23*).

The structural basis of the possible coevolution of ribonucleases and RI (Figure 1A) has been elucidated at atomic resolution for four RNase A superfamily members: RNase A, angiogenin (RNase 5), eosinophil-derived neurotoxin (RNase 2), and RNase 1 (*28*−*30*, *73*, *74*). The structural contacts within the hRI·RNase 1 complex (PDB accession

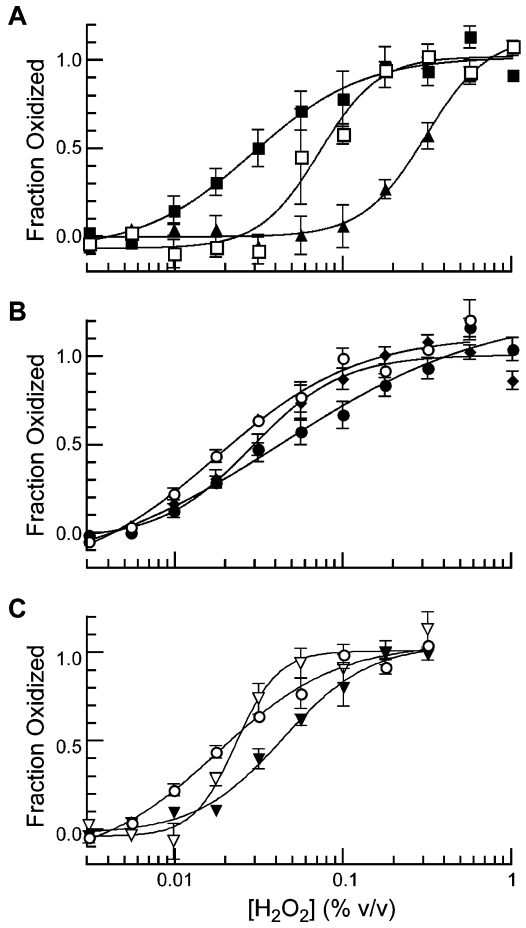

FIGURE 4: Stability to hydrogen peroxide oxidation (H_2O_2) of RI and RI·ribonuclease complexes. The decrease in fluorescence intensity of diethylfluorescein-labeled ribonuclease upon binding to RI was used to measure the oxidative stability of free RI and RI·ribonuclease complexes (*36*, *38*, *44*). The complex formed by RI (10 μM) and ribonuclease (10 μM) was incubated in serial dilutions of H_2O_2 buffered in 20 mM HEPES−HCl buffer, pH 7.6, containing KCl (50 mM) and DTT (≤50 μM) for 30 min at 37 °C. Data points are the mean (±SE) of three independent experiments and were normalized for the maximum fluorescence of the unbound ribonuclease. Data were fitted to eq 2 to determine values of IC_{50} (Table 1). Panel A depicts data for bRI (□), bRI·RNase A (▲), and bRI·RNase 1 (■); panel B depicts data for hRI (○), hRI·RNase 1 (◆), and hRI·RNase A (●); panel C depicts data for hRI (○), C74L hRI (▼), and C408G hRI (▽).

code 1Z7X) were extracted and the conservation of these RI residues are compared in Table 2 (*28*). If RI and ribonuclease have coevolved, contact residues are likely to be conserved between RI proteins. For example, bRI and chicken RI have amino acid sequence identities to hRI of 74 and 49%, respectively (Figure S-1), but for contact residues, the sequence identities to hRI are 93 and 61%, respectively (Table 2). The greater conservation of contact residues is consistent with the existence of selective pressure that maintains the high affinity of RI for ribonucleases. Also, a phylogenetic tree of these RI proteins from diverse organisms (Figure 5A) has an architecture and rate of evolution similar to that of the phylogenetic tree of ribonucleases from the same organisms (Figure 5B) (*52*−*54*). To gain insight into the coevolution of affinity of this femtomolar protein−protein complex and to address whether an evolutionary imperative exists for species-specific regulation of ribonucleolytic activity, RI from cow and human were produced in *E. coli* and purified along with their cognate ribonucleases.

Table 2: Conservation of Ribonuclease-Contact Residues in RIs[a]

human	chimp	cow	pig	mouse	rat	chicken
Q10	Q	Q	H	Q	Q	Q
C11	C	C	C	C	C	C
R33	R	R	R	R	R	R
R35	D	D	D	D	D	D
D36	D	D	D	D	D	D
W261	W	W	W	W	W	W
W263	W	W	W	W	W	W
E264	E	E	E	E	D	D
E287	E	E	E	E	E	E
A291	A	A	A	A	A	I
G292	G	G	G	S	G	D
K320	K	K	K	K	K	R
W375	W	W	C	W	W	W
E401	E	E	E	E	E	E
N406	N	N	N	N	N	Y
N407	N	N	N	N	N	N
C408	C	G	C	C	C	T
L409	L	L	V	M	M	L
G410	G	G	G	G	G	E
Q430	Q	Q	Q	Q	Q	Q
Y434	Y	Y	Y	Y	Y	Y
D435	D	D	D	D	D	D
Y437	Y	Y	Y	Y	Y	F
W438	W	W	W	W	W	W
S439	S	T	T	T	T	G
E440	E	E	E	N	D	P
R457	R	R	R	R	R	K
S460	S	S	S	S	S	S

[a] Contact residues in the hRI·RNase 1 complex are from PDB accession code 1Z7X (chains Y and Z) (*28*). RI residues from other organisms are from the alignment in Figure S-2.

The binding of proteins to small ligands can increase the thermal stability of the protein through the influence of the ligand on the unfolding equilibrium of the protein (*58*, *59*, *61*, *64*). The increase in thermal stability (ΔT_m) can be related directly to the binding affinity (K_d) of ligands for the protein (*75*) but only when the association rate and binding enthalpy of the ligands are constant (*64*). These same principles of thermal stabilization can also be applied to protein·protein complexes (*62*, *63*). Both RI and ribonuclease are stabilized upon formation of a RI·ribonuclease complex (Table 1). All of the complexes between bRI or hRI and ribonuclease have $\Delta T_m > 10$ °C from free RI, with the bRI·RNase A complex having the largest change at 17−18 °C. This ΔT_m value is similar to that for barstar upon complex formation with barnase ($\Delta T_m = 20$ °C (*63*)), its cognate ribonuclease. Like the binding of vertebrate ribonucleases by RI, the binding of barnase by barstar is essential to cell survival (*76*). Thus, all known essential ribonuclease inhibitor−ribonuclease interactions have a ΔT_m value in the range of 10−20 °C.

For RI·ribonuclease complexes, ΔT_m should serve as a good indicator of binding affinity (*64*, *75*), as the association rates and binding enthalpies for RNase 1 and RNase A should be nearly identical (*28*). The dissociation rate constants and ΔT_m for RI·ribonuclease complexes do indeed correlate, as the hRI·RNase A complex has the fastest dissociation rate and the lowest ΔT_m (10 °C), and as both bRI·ribonuclease complexes have identical k_d values and ΔT_m values (Table 1). This direct relationship between binding affinity and thermal stability suggests that the thermal stability of RI·ribonuclease complexes could be used in future studies to estimate their binding affinities.

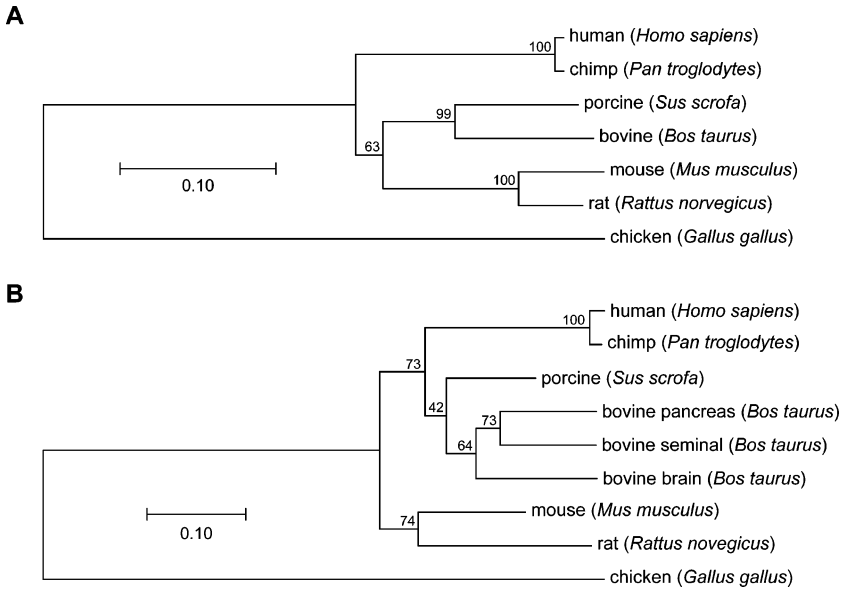

FIGURE 5: Phylogenetic tree of RIs (A) and ribonucleases (B) from various organisms. Cladograms of RI and ribonuclease were made with the program MegAlign from the Lasergene software package (DNASTAR, Madison, WI). Bootstrap values were calculated using 2000 replicates, and values >40 are reported. The bar indicates the distance for 0.10 substitutions per site. GenBank accession codes for RI and ribonuclease sequences are listed in the experimental procedures, and sequence alignments are shown in Figures S-2 and S-3.

Besides acting as an intracellular sentry, RI appears to play another biological role. The natural abundance of cysteine residues is 1.7% (*77*). In contrast, 6−7% of the residues in known RIs are cysteine. The 29−32 cysteine residues of RI are able to contribute to the regulation of cellular redox homeostasis by scavenging free radicals (*47*, *48*, *78*). The ensuing oxidation of the cysteine residues to half-cystines leads to the rapid degradation of RI in the cell (*78*). In primates, RI seems to have evolved greater sensitivity to oxidation through the addition of a specific cysteine residue, Cys74 (Figure 4C), whose conversion to leucine increases the oxidative stability of hRI by 2.5-fold. This increased sensitivity of hRI to oxidation could facilitate greater regulation of the cellular concentration of hRI through modulation of the cellular redox environment and thus permit more sensitive control over ribonuclease biology.

Upon formation of a complex with an intraspecies ribonuclease, the oxidative stability of RI increases (Table 1 and Figure 4), compromising its ability to compensate for oxidative stress. Apparently, the two biological roles of RI are functionally distinct, but its role in inhibiting invading ribonucleases appears to supersede its role in mediating oxidative damage, as even under extreme oxidative stress (e.g., 0.13 M H_2O_2 for the bRI·RNase A complex), it remains bound to ribonucleases. Other cellular biomolecules can serve to regulate the cellular redox environment (*79*), but no other cellular inhibitors of ribonucleases are known (*26*). Consequently, RI needs to maintain its high affinity for ribonucleases so as to protect cellular RNA, even under severely oxidizing conditions (*12*, *13*, *15*).

The kinetic inhibition of ribonucleases by RI is essentially permanent, as both bRI and hRI bind RNase A and RNase 1 with K_d values that are below 35 fM and with $t_{1/2}$ values for the complexes (except the hRI·RNase A complex) that extend beyond 5 weeks (Table 1). Interestingly, bRI does not show the same species-specific affinity preference of hRI (*28*). Rather, bRI maintains broader specificity for ribonucleases (Table 1 and Figure 2) and greater oxidative stability than hRI (Figure 4). Cows have more ribonucleases (20 (*22*)) than do humans (13 (*21*)), including three with high similarity to RNase 1 from three different tissues (Figure 5B). Accordingly, bRI might need to maintain broader specificity so as to recognize more ribonucleases. Additionally, the biological role of RNase A is to digest dietary RNA in a cow stomach (*80*), but new biological roles for RNase 1 in vertebrates seem to be evolving, as bursts of gene duplication and gene deactivation are observed in *Carnivora* (*81*). hRI might be evolving new biological roles along with RNase 1 and adding new levels of cellular regulation through its sensitivity to oxidative stress. Addressing these evolutionary questions will require the purification and identification of RI proteins from additional organisms and performing analyses similar to those performed for ribonucleases (*17*, *18*, *21*, *22*, *82*).

Conclusions. The complexes between RI and ribonucleases serve as an ideal model system to investigate the coevolution of an essentially permanent protein−protein complex. To protect cells from damaging ribonucleolytic activity, the RI·ribonuclease complex remains intact even when confronted by severe thermal or oxidative stress. Yet, hRI shows increased sensitivity to oxidation (largely due to Cys74) than does bRI, suggesting greater regulation of the cellular concentration of hRI through modulation of the cellular redox environment. hRI also displays greater variation in binding affinity for ribonucleases, as it binds RNase 1 with significantly higher affinity than RNase A, whereas bRI maintains broader specificity, binding both ribonucleases with high affinity.

ACKNOWLEDGMENT

We are grateful to D. R. McCaslin for assistance with CD spectroscopy, and to T. J. Rutkoski and G.A. Ellis for assistance with RI purification.

SUPPORTING INFORMATION AVAILABLE

Sequence identities for RIs and ribonucleases shown in Figure 5 (Figure S-1), multiple sequence alignment of RIs for Figure 5A (Figure S-2), and multiple sequence alignment of ribonucleases for Figure 5B (Figure S-3). This material is available free of charge via the Internet at http://pubs.acs.org

REFERENCES

1. Gavin, A. C., Bosche, M., Krause, R., Grandi, P., Marzioch, M., Bauer, A., Schultz, J., Rick, J. M., Michon, A. M., Cruciat, C. M., Remor, M., Hofert, C., Schelder, M., Brajenovic, M., Ruffner, H., Merino, A., Klein, K., Hudak, M., Dickson, D., Rudi, T., Gnau, V., Bauch, A., Bastuck, S., Huhse, B., Leutwein, C., Heurtier, M. A., Copley, R. R., Edelmann, A., Querfurth, E., Rybin, V., Drewes, G., Raida, M., Bouwmeester, T., Bork, P., Seraphin, B., Kuster, B., Neubauer, G., and Superti-Furga, G. (2002) Functional organization of the yeast proteome by systematic analysis of protein complexes, *Nature 415*, 141−147.
2. Ho, Y., Gruhler, A., Heilbut, A., Bader, G. D., Moore, L., Adams, S. L., Millar, A., Taylor, P., Bennett, K., Boutilier, K., Yang, L., Wolting, C., Donaldson, I., Schandorff, S., Shewnarane, J., Vo, M., Taggart, J., Goudreault, M., Muskat, B., Alfarano, C., Dewar, D., Lin, Z., Michalickova, K., Willems, A. R., Sassi, H., Nielsen, P. A., Rasmussen, K. J., Andersen, J. R., Johansen, L. E., Hansen, L. H., Jespersen, H., Podtelejnikov, A., Nielsen, E., Crawford, J., Poulsen, V., Sorensen, B. D., Matthiesen, J., Hendrickson, R. C., Gleeson, F., Pawson, T., Moran, M. F., Durocher, D., Mann, M., Hogue, C. W., Figeys, D., and Tyers, M. (2002) Systematic identification of protein complexes in *Saccharomyces cerevisiae* by mass spectrometry, *Nature 415*, 180−183.
3. Krogan, N. J., Cagney, G., Yu, H., Zhong, G., Guo, X., Ignatchenko, A., Li, J., Pu, S., Datta, N., Tikuisis, A. P., Punna, T., Peregrin-Alvarez, J. M., Shales, M., Zhang, X., Davey, M., Robinson, M. D., Paccanaro, A., Bray, J. E., Sheung, A., Beattie, B., Richards, D. P., Canadien, V., Lalev, A., Mena, F., Wong, P., Starostine, A., Canete, M. M., Vlasblom, J., Wu, S., Orsi, C., Collins, S. R., Chandran, S., Haw, R., Rilstone, J. J., Gandi, K., Thompson, N. J., Musso, G., St. Onge, P., Ghanny, S., Lam, M. H., Butland, G., Altaf-Ul, A. M., Kanaya, S., Shilatifard, A., O'Shea, E., Weissman, J. S., Ingles, C. J., Hughes, T. R., Parkinson, J., Gerstein, M., Wodak, S. J., Emili, A., and Greenblatt, J. F. (2006) Global landscape of protein complexes in the yeast *Saccharomyces cerevisiae*, *Nature 440*, 637−643.
4. Fraser, H. B., Hirsh, A. E., Steinmetz, L. M., Scharfe, C., and Feldman, M. W. (2002) Evolutionary rate in the protein interaction network, *Science 296*, 750−752.
5. Lemos, B., Meiklejohn, C. D., and Hartl, D. L. (2004) Regulatory evolution across the protein interaction network, *Nat. Genet. 36*, 1059−1060.
6. Hahn, M. W., and Kern, A. D. (2005) Comparative genomics of centrality and essentiality in three eukaryotic protein-interaction networks, *Mol. Biol. Evol. 22*, 803−806.
7. Mintseris, J., and Weng, Z. (2005) Structure, function, and evolution of transient and obligate protein−protein interactions, *Proc. Natl. Acad. Sci. U.S.A. 102*, 10930−10935.
8. Saeed, R., and Deane, C. M. (2006) Protein−protein interactions, evolutionary rate, abundance and age, *BMC Bioinformatics 7*, 128.
9. Liao, B. Y., Scott, N. M., and Zhang, J. (2006) Impacts of gene essentiality, expression pattern, and gene compactness on the evolutionary rate of mammalian proteins, *Mol. Biol. Evol. 23*, 2072−2080.
10. He, X., and Zhang, J. (2006) Why do hubs tend to be essential in protein networks, *PLoS Genet. 2*, e88.
11. Nooren, I. M., and Thornton, J. M. (2003) Diversity of protein−protein interactions, *EMBO J. 22*, 3486−3492.
12. Raines, R. T. (1998) Ribonuclease A, *Chem. Rev. 98*, 1045−1065.
13. Leland, P. A., Schultz, L. W., Kim, B.-M., and Raines, R. T. (1998) Ribonuclease A variants with potent cytotoxic activity, *Proc. Natl. Acad. Sci. U.S.A. 98*, 10407−10412.
14. Leland, P. A., and Raines, R. T. (2001) Cancer chemotherapy−ribonucleases to the rescue, *Chem. Biol. 8*, 405−413.
15. Smith, B. D., and Raines, R. T. (2006) Genetic selection for critical residues in ribonucleases, *J. Mol. Biol. 362*, 459−478.
16. Beintema, J. J. (1987) Structure, properties and molecular evolution of pancreatic-type ribonucleases, *Life Chem. Rep. 4*, 333−389.
17. Beintema, J. J., Schüller, C., Irie, M., and Carsana, A. (1988) Molecular evolution of the ribonuclease superfamily, *Prog. Biophys. Mol. Biol. 51*, 165−192.
18. Beintema, J. J., Breukelman, H. J., Carsana, A., and Furia, A. (1997) Evolution of vertebrate ribonucleases: Ribonuclease A superfamily, in *Ribonucleases: Structures and Functions* (D'Alessio, G., and Riordan, J. F., Eds.), pp 245−269, Academic Press, New York.
19. Zhang, J., Rosenberg, H. F., and Nei, M. (1998) Positive Darwinian selection after gene duplication in primate ribonuclease genes, *Proc. Natl. Acad. Sci. U.S.A. 95*, 3708−3713.
20. Singhania, N. A., Dyer, K. D., Zhang, J., Deming, M. S., Bonville, C. A., Domachowske, J. B., and Rosenberg, H. F. (1999) Rapid evolution of the ribonuclease A superfamily: Adaptive expansion of independent gene clusters in rats and mice, *J. Mol. Evol. 49*, 721−728.
21. Cho, S., Beintema, J. J., and Zhang, J. (2005) The ribonuclease A superfamily of mammals and birds: Identifying new members and tracing evolutionary histories, *Genomics 85*, 208−220.
22. Cho, S., and Zhang, J. (2006) Ancient expansion of the ribonuclease A superfamily revealed by genomic analysis of placental and marsupial mammals, *Gene 373*, 116−125.
23. Pizzo, E., Buonanno, P., Di Maro, A., Ponticelli, S., De Falco, S., Quarto, N., Cubellis, M. V., and D'Alessio, G. (2006) Ribonucleases and angiogenins from fish, *J. Biol. Chem. 281*, 27454−27460.
24. Nitto, T., Dyer, K. D., Czapiga, M., and Rosenberg, H. F. (2006) Evolution and function of leukocyte RNase A ribonucleases of the avian species, *Gallus gallus*, *J. Biol. Chem. 281*, 25622−25634.
25. Haigis, M. C., Kurten, E. L., and Raines, R. T. (2003) Ribonuclease inhibitor as an intracellular sentry, *Nucleic Acids Res. 31*, 1024−1032.
26. Dickson, K. A., Haigis, M. C., and Raines, R. T. (2005) Ribonuclease inhibitor: Structure and function, *Prog. Nucleic Acid Res. Mol. Biol. 80*, 349−374.
27. Lee, F. S., Shapiro, R., and Vallee, B. L. (1989) Tight-binding inhibition of angiogenin and ribonuclease A by placental ribonuclease inhibitor, *Biochemistry 28*, 225−230.
28. Johnson, R. J., McCoy, J. G., Bingman, C. A., Phillips, G. N., Jr., and Raines, R. T. (2007) Inhibition of human pancreatic ribonuclease by the human ribonuclease inhibitor protein, *J. Mol. Biol. 368*, 434−449.
29. Kobe, B., and Deisenhofer, J. (1995) A structural basis of the interactions between leucine-rich repeats and protein ligands, *Nature 374*, 183−186.
30. Kobe, B., and Deisenhofer, J. (1996) Mechanism of ribonuclease inhibition by ribonuclease inhibitor protein based on the crystal structure of its complex with ribonuclease A, *J. Mol. Biol. 264*, 1028−1043.
31. Haigis, M. C., Haag, E. S., and Raines, R. T. (2002) Evolution of ribonuclease inhibitor protein by exon duplication, *Mol. Biol. Evol. 19*, 960−964.
32. Smith, B. D., Soellner, M. B., and Raines, R. T. (2003) Potent inhibition of ribonuclease A by oligo(vinylsulfonic acid), *J. Biol. Chem. 278*, 20934−20938.
33. Rutkoski, T. J., Kurten, E. L., Mitchell, J. C., and Raines, R. T. (2005) Disruption of shape-complementarity markers to create cytotoxic variants of ribonuclease A, *J. Mol. Biol. 354*, 41−54.
34. Klink, T. A., Vicentini, A. M., Hofsteenge, J., and Raines, R. T. (2001) High-level soluble production and characterization of porcine ribonuclease inhibitor, *Protein Expr. Purif. 22*, 174−179.
35. Lavis, L. D., Chao, T.-Y., and Raines, R. T. (2006) Fluorogenic label for biomolecular imaging, *ACS Chem. Biol. 1*, 252−260.
36. Abel, R. L., Haigis, M. C., Park, C., and Raines, R. T. (2002) Fluorescence assay for the binding of ribonuclease A to the ribonuclease inhibitor protein, *Anal. Biochem. 306*, 100−107.
37. Riddles, P. W., Blakeley, R. L., and Zerner, B. (1983) Reassessment of Ellman's reagent, *Methods Enzymol. 91*, 49−60.
38. Lavis, L. D., Rutkoski, T. J., and Raines, R. T. (2007) Tuning the pK_a of fluorescein to optimize binding assays, *Anal. Chem. 79*, 6755−6782.
39. Leland, P. A., Staniszewski, K. E., Park, C., Kelemen, B. R., and Raines, R. T. (2002) The ribonucleolytic activity of angiogenin, *Biochemistry 41*, 1343−1350.

40. Johnson, R. J., Lin, S. R., and Raines, R. T. (2006) A ribonuclease zymogen activated by the NS3 protease of the hepatitis C virus, *FEBS J. 273*, 5457−5465.
41. Johnson, R. J., Lin, S. R., and Raines, R. T. (2007) Genetic selection to reveal the role of a buried, conserved polar residue, *Protein Sci. 16*, 1609−1616.
42. Pace, C. N. (1990) Measuring and increasing protein stability, *Trends Biotechnol. 8*, 93−98.
43. Pace, C. N., Hebert, E. J., Shaw, K. L., Schell, D., Both, V., Krajcikova, D., Sevcik, J., Wilson, K. S., Dauter, Z., Hartley, R. W., and Grimsley, G. R. (1998) Conformational stability and thermodynamics of folding of ribonucleases Sa, Sa2 and Sa3, *J. Mol. Biol. 279*, 271−286.
44. Kim, B.-M., Schultz, L. W., and Raines, R. T. (1999) Variants of ribonuclease inhibitor that resist oxidation, *Protein Sci. 8*, 430−434.
45. Chenna, R., Sugawara, H., Koike, T., Lopez, R., Gibson, T. J., Higgins, D. G., and Thompson, J. D. (2003) Multiple sequence alignment with the Clustal series of programs, *Nucleic Acids Res. 31*, 3497−3500.
46. McEwan, P. A., Scott, P. G., Bishop, P. N., and Bella, J. (2006) Structural correlations in the family of small leucine-rich repeat proteins and proteoglycans, *J. Struct. Biol. 155*, 294−305.
47. Wang, S., and Li, H. (2006) Radical scavenging activity of ribonuclease inhibitor from cow placenta, *Biochemistry (Moscow) 71*, 520−524.
48. Monti, D. M., Montesano Gesualdi, N., Matoušek, J., Esposito, F., and D'Alessio, G. (2007) The cytosolic ribonuclease inhibitor contributes to intracellular redox homeostasis, *FEBS Lett. 581*, 930−934.
49. Park, C., and Raines, R. T. (2001) Adjacent cysteine residues as a redox switch, *Protein Eng. 14*, 939−942.
50. Burton, L. E., Blackburn, P., and Moore, S. (1980) Ribonuclease inhibitor from bovine brain, *Int. J. Pept. Protein Res. 16*, 359−364.
51. Burton, L. E., and Fucci, N. P. (1982) Ribonuclease inhibitors from the livers of five mammalian species, *Int. J. Pept. Protein Res. 19*, 372−379.
52. Hofsteenge, J., Kieffer, B., Matthies, R., Hemmings, B. A., and Stone, S. R. (1988) Amino acid sequence of the ribonuclease inhibitor from porcine liver reveals the presence of leucine-rich repeats, *Biochemistry 27*, 8537−8544.
53. Lee, F. S., Fox, E. A., Zhou, H.-M., Strydom, D. J., and Vallee, B. L. (1988) Primary structure of human placental ribonuclease inhibitor, *Biochemistry 27*, 8545−8553.
54. Kawanomoto, M., Motojima, K., Sasaki, M., Hattori, H., and Goto, S. (1992) cDNA cloning and sequence of rat ribonuclease inhibitor, and tissue distribution of mRNA, *Biochim. Biophys. Acta 1129*, 335−338.
55. Teufel, D. P., Kao, R. Y., Acharya, K. R., and Shapiro, R. (2003) Mutational analysis of the complex of human RNase inhibitor and human eosinophil-derived neurotoxin (RNase 2), *Biochemistry 42*, 1451−1459.
56. Stone, S. R., and Hofsteenge, J. (1986) Kinetics of the inhibition of thrombin by hirudin, *Biochemistry 25*, 4622−4628.
57. Shaul, Y., and Schreiber, G. (2005) Exploring the charge space of protein−protein association: A proteomic study, *Proteins 60*, 341−352.
58. Sturtevant, J. M. (1987) Biochemical applications of differential scanning calorimetry, *Annu. Rev. Phys. Chem. 38*, 463−488.
59. Brandts, J. F., and Lin, L. N. (1990) Study of strong to ultratight protein interactions using differential scanning calorimetry, *Biochemistry 29*, 6927−6940.
60. Hytönen, V. P., Nyholm, T. K., Pentikäinen, O. T., Vaarno, J., Porkka, E. J., Nordlund, H. R., Johnson, M. S., Slotte, J. P., Laitinen, O. H., and Kulomaa, M. S. (2004) Chicken avidin-related protein 4/5 shows superior thermal stability when compared with avidin while retaining high affinity to biotin, *J. Biol. Chem. 279*, 9337−9343.
61. Mayhood, T. W., and Windsor, W. T. (2005) Ligand binding affinity determined by temperature-dependent circular dichroism: Cyclin-dependent kinase 2 inhibitors, *Anal. Biochem. 345*, 187−197.
62. Donovan, J. W., and Beardslee, R. A. (1975) Heat stabilization produced by protein−protein association. A differential scanning calorimetric study of the heat denaturation of the trypsin−soybean trypsin inhibitor and trypsin−ovomucoid complexes, *J. Biol. Chem. 250*, 1966−1971.
63. Makarov, A. A., Protasevich, I. I., Lobachov, V. M., Kirpichnikov, M. P., Yakovlev, G. I., Gilli, R. M., Briand, C. M., and Hartley, R. W. (1994) Thermostability of the barnase−barstar complex, *FEBS Lett. 354*, 251−254.
64. Waldron, T. T., and Murphy, K. P. (2003) Stabilization of proteins by ligand binding: Application to drug screening and determination of unfolding energetics, *Biochemistry 42*, 5058−5064.
65. Kelly, S. M., Jess, T. J., and Price, N. C. (2005) How to study proteins by circular dichroism, *Biochim. Biophys. Acta 1751*, 119−139.
66. Cavallo, L., Kleinjung, J., and Fraternali, F. (2003) POPS: A fast algorithm for solvent accessible surface areas at atomic and residue level, *Nucleic Acids Res. 31*, 3364−3366.
67. Johnson, R. J., Chao, T.-Y., Lavis, L. D., and Raines, R. T. (2007) Cytotoxic ribonucleases: The dichotomy of Coulombic forces, *Biochemistry 46*, 10308−10316.
68. Szajewski, R. P., and Whitesides, G. M. (1980) Rate constants and equilibrium constants for thiol−disulfide interchange reactions involving oxidized glutathione, *J. Am. Chem. Soc. 102*, 2011−2026.
69. Shaked, Z., Szajewski, R. P., and Whitesides, G. M. (1980) Rates of thiol−disulfide interchange reactions involving proteins and kinetic measurements of thiol pK_a values, *Biochemistry 19*, 4156−4166.
70. Leland, P. A., Staniszewski, K. E., Kim, B.-M., and Raines, R. T. (2001) Endowing human pancreatic ribonuclease with toxicity for cancer cells, *J. Biol. Chem. 276*, 43095−43102.
71. Tomita, Y., Goto, Y., Okazaki, T., and Shukuya, R. (1979) Liver ribonucleases from the bullfrog, *Rana catesbeiana*. Purification, properties and changes in activity during metamorphosis, *Biochim. Biophys. Acta 562*, 504−514.
72. Wu, Y., Mikulski, S. M., Ardelt, W., Rybak, S. M., and Youle, R. J. (1993) A cytotoxic ribonuclease, *J. Biol. Chem. 268*, 10686−10693.
73. Papageorgiou, A., Shapiro, R., and Acharya, K. (1997) Molecular recognition of human angiogenin by placental ribonuclease inhibitor—an X-ray crystallographic study at 2.0 Å resolution, *EMBO J. 16*, 5162−5177.
74. Iyer, S., Holloway, D. E., Kumar, K., Shapiro, R., and Acharya, K. R. (2005) Molecular recognition of human eosinophil-derived neurotoxin (RNase 2) by placental ribonuclease inhibitor, *J. Mol. Biol. 347*, 637−655.
75. Matulis, D., Kranz, J. K., Salemme, F. R., and Todd, M. J. (2005) Thermodynamic stability of carbonic anhydrase: Measurements of binding affinity and stoichiometry using ThermoFluor, *Biochemistry 44*, 5258−5266.
76. Hartley, R. W. (1989) Barnase and barstar: Two small proteins to fold and fit together, *Trends Biochem. Sci. 14*, 450−454.
77. McCaldon, P., and Argos, P. (1988) Oligopeptide biases in protein sequences and their use in predicting protein coding regions in nucleotide sequences, *Proteins 4*, 99−122.
78. Blázuez, M., Fominaya, J. M., and Hofsteenge, J. (1996) Oxidation of sulfhydryl groups of ribonuclease inhibitor in epithelial cells is sufficient for its intracellular degradation, *J. Biol. Chem. 271*, 18638−18642.
79. Valko, M., Rhodes, C. J., Moncol, J., Izakovic, M., and Mazur, M. (2006) Free radicals, metals and antioxidants in oxidative stress-induced cancer, *Chem. Biol. Interact. 160*, 1−40.
80. Barnard, E. A. (1969) Biological function of pancreatic ribonuclease, *Nature 221*, 340−344.
81. Yu, L., and Zhang, Y. P. (2006) The unusual adaptive expansion of pancreatic ribonuclease gene in carnivora, *Mol. Biol. Evol. 23*, 2326−2335.
82. Beintema, J. J., Hofsteenge, J., Iwama, M., Morita, T., Ohgi, K., Irie, M., Sugiyama, R. H., Schieven, G. L., Dekker, C. A., and Glitz, D. G. (1988) Amino acid sequence of the nonsecretory ribonuclease of human urine, *Biochemistry 27*, 4530−4538.

BI701521Q